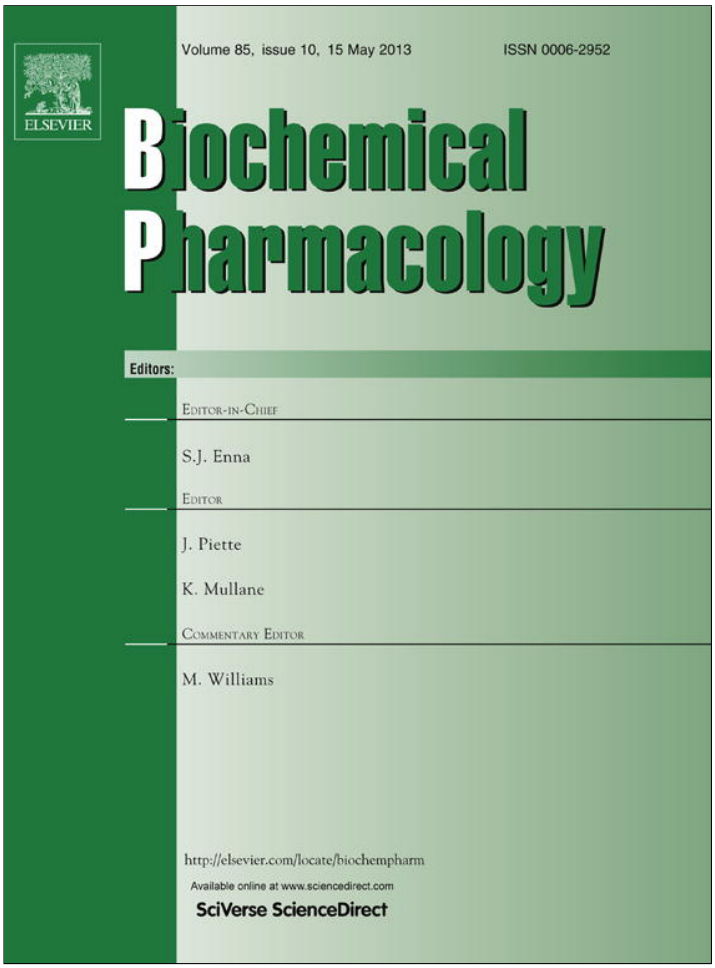

Biochemical Pharmacology 85 (2013) 1534–1541

Contents lists available at SciVerse ScienceDirect

Biochemical Pharmacology

journal homepage: www.elsevier.com/locate/biochempharm

α_1-Adrenoceptor and serotonin 5-HT_{1A} receptor affinity of homobivalent 4-aminoquinoline compounds: An investigation of the effect of linker length

Junli Chen [a], Ahsan K. Murad [a], Laurence P.G. Wakelin [a], William A. Denny [b], Renate Griffith [a], Angela M. Finch [a,*]

[a] Department of Pharmacology, School of Medical Sciences, UNSW, Sydney, NSW 2052, Australia
[b] Auckland Cancer Society Research Centre, Faculty of Medicine and Health Science, University of Auckland, 1142, New Zealand

ARTICLE INFO

Article history:
Received 18 January 2013
Accepted 13 March 2013
Available online 19 March 2013

Keywords:
GPCR
α_1-Adrenergic receptor
Subtype selectivity
Serotonin receptor
Diquinoline
Linker length

ABSTRACT

α_1-adrenoceptor (α_1-AR) subtype-selective ligands lacking off-target affinity for the 5-HT_{1A} receptor (5-HT_{1A}-R) will provide therapeutic benefits in the treatment of urogenital conditions such as benign prostatic hyperplasia. In this study we determined the affinity of 4-aminoquinoline and eleven homobivalent 4-aminoquinoline ligands (diquinolines) with alkane linkers of 2–12 atoms (C2–C12) for α_{1A}, α_{1B} and α_{1D} -ARs and the 5-HT_{1A}-R. These ligands are α_{1A}-AR antagonists with nanomolar affinity for α_{1A} and α_{1B} -ARs. They display linker-length dependent selectivity for $\alpha_{1A/B}$ -ARs over α_{1D}-AR and the 5-HT_{1A}-R. The C2 diquinoline has the highest affinity for α_{1A}-AR (pK_i 7.60 ± 0.26) and greater than 30-fold and 600-fold selectivity for α_{1A}-AR over α_{1D}-AR and 5-HT_{1A}-R respectively. A decrease in affinity for α_1-ARs is observed as the linker length increases, reaching a nadir at 5 ($\alpha_{1A/1B}$-ARs) or 6 (α_{1D}-AR) atoms; after which affinity increases as the linker is lengthened, peaking at 9 ($\alpha_{1A/1B/1D}$-ARs) or 8 (5-HT_{1A}-R) atoms. Docking studies suggest that 4-aminoquinoline and C2 bind within the orthosteric binding site, while for C9 one end is situated within the orthosteric binding pocket, while the other 4-aminoquinoline moiety interacts with the extracellular surface. The limited α_{1D}-AR and 5-HT_{1A}-R affinity of these compounds makes them promising leads for future drug development of α_{1A}-AR selective ligands without α_{1D}-AR and the 5-HT_{1A}-R off-target activity.

1. Introduction

α_1-adrenoceptors (α_1-ARs) are members of the seven-transmembrane-spanning G-protein-coupled receptor (GPCR) superfamily, and exist as three distinct subtypes: α_{1A}, α_{1B} and α_{1D}. α_1-ARs respond to the endogenous catecholamines, norepinephrine and epinephrine, and play a vital role in numerous physiological functions predominantly involving smooth muscle contraction, which makes them a therapeutic target for several urogenital conditions, such as benign prostatic hyperplasia (BPH) and stress urinary retention [1,2]. BPH is a widespread condition in males over 60 with the incidence of this condition increasing as men age. One of the most effective treatments for BPH is therapy with α_1-AR antagonists (ideally α_{1A}-AR antagonists, as this is the predominant subtype in the urogenital tract) [1]. Antagonism of the α_1-AR prevents the contraction of the smooth muscle of the prostate gland and the bladder neck, thus decreasing lower urinary tract symptoms of BPH [1]. The α_1-AR antagonists that are used currently have similar therapeutic outcomes but have different side effect profiles due to the lack of subtype selectivity, and off-target affinity. For example, alfuzosin and terazosin have equal affinity for each of the α_1-AR subtypes: this can result in cardiovascular side effects such as hypotension mediated by the α_{1B}-AR, the predominant subtype in the blood vessels of older men [3]. In contrast, tamsulosin and naftopidil have higher affinity for α_{1A} and α_{1D}-ARs than for α_{1B}-AR and hence reduced cardiovascular side effects. However, they also have nanomolar affinity for the serotonin 5-HT_{1A} receptor (5-HT_{1A}-R), and tamsulosin has nanomolar affinity for the dopamine D_3 receptor (D_3-R) [4,5]. The high off-target affinity of tamsulosin and naftopidil has been implicated in floppy iris syndrome and ejaculatory dysfunction side effects [4,6].

Previously, a series of homobivalent 4-aminoquinoline compounds (diquinolines) was shown to have high affinity for rat α_1-adrenoceptors [7,8], with tissue-specific differences. However,

* Corresponding author at: School of Medical Sciences, Wallace Wurth Building, University of New South Wales, NSW 2052, Australia. Tel.: +61 293851325.
E-mail addresses: junli.chen@unsw.edu.au (J. Chen), m.a.murad@unsw.edu.au (A.K. Murad), l.wakelin@unsw.edu.au (Laurence P.G. Wakelin), b.denny@auckland.ac.nz (W.A. Denny), r.griffith@unsw.edu.au (R. Griffith), a.finch@unsw.edu.au (A.M. Finch).

0006-2952/$ – see front matter © 2013 Elsevier Inc. All rights reserved.
http://dx.doi.org/10.1016/j.bcp.2013.03.010

at that time the α_1-AR had not been classified into the current three subtypes, therefore the subtype selectivity of these compounds was not determined. In this study, we find that the diquinolines show nano- to micro-molar affinity and a similar linker length-affinity relationship for each α_1-AR subtype. Five of the compounds (C2, C3, C5, C6 and C12) have significantly higher affinity for α_{1A}-AR over α_{1D}-AR and all compounds, with the exception of 4-aminoquinoline, C7, and C3 amine, display significant selectivity for α_{1A}-AR over 5-HT_{1A}-R.

2. Materials and methods

The diquinolines were prepared and isolated as their dihydrochloride salts as previously described [7,8]. C2, C3, C5 and C6 diquinoline were dissolved in ultra-pure water (Millipore, Billerica, MA, USA) at 10 mM, and C7, C8, C9, C10, C11 and C12 were solubilised at 10 mM in 90% dimethyl sulphoxide/water (DMSO). These stock solutions were stored at −80 °C. Dulbecco's modified Eagle's medium (DMEM), fetal bovine serum (FBS), L-glutamine, penicillin and streptomycin were purchased from Thermo Fisher Scientific (Scoresby, VIC, Australia). [^{3}H] prazosin (85 Ci mmol^{-1}) and [^{3}H]-myo-inositol (20 Ci mmol^{-1}) were purchased from PerkinElmer (Waltham, MA, USA) and [^{3}H]-OH-DPAT (226 Ci mmol^{-1}) from GE Healthcare (Uppsala, Sweden). Phentolamine hydrochloride, serotonin hydrochloride, norepinephrine hydrochloride, diethylaminoethyl-dextran (DEAE-dextran), lithium chloride (LiCl), formic acid, ammonium formate and chemicals used in buffered solutions (HEPES, EGTA and $MgCl_2$) were bought from Sigma–Aldrich (St. Louis, MO, USA), and Tris, $CaCl_2$, NaCl, KCl, Na_2HPO_4, and KH_2PO_4 were purchased from Ajax Finechem (Taren Point, NSW, Australia).

2.1. Cell culture and transient transfection

COS-1 cells (American Type Culture Collection, Manassas, VA, USA) were cultured in DMEM supplemented with 10% (v/v) heat-inactivated FBS, 100 μg ml^{-1} penicillin and 100 μg ml^{-1} streptomycin. COS-1 cells were maintained and passaged upon reaching confluence using standard cell culture techniques and replaced by lower passage number cells upon nearing 50 passage cycles. Transient transfection of human α_{1A} and α_{1B} -ARs and 5-HT_{1A}-R was performed using pcDNA 3.1+ vectors containing inserted cDNA for each of the receptors (Missouri S&T cDNA resource center, MO, USA), and for the human α_{1D}-AR via pMV6-XL5 vector (Origene, Rockville, MO, USA) containing inserted α_{1D}-AR cDNA. The DEAE-dextran methodology was used to perform the transfection as previously described [9].

2.2. Membrane preparation

Membrane suspensions were formed from COS-1 cells transiently transfected with the cDNA of interest, as previously described [10]. Cells were scraped from the surface of culture plates, suspended in phosphate-buffered saline, and then centrifuged at 1000 × *g* for 5 min. The pellet was resuspended in 10 mL 0.25 M sucrose containing protease inhibitors, disrupted, and homogenized by 10–15 strokes with a tight-fitting pestle in a Dounce homogenizer. Nuclear debris was removed by centrifugation at 1260 g for 5 min. The membrane pellet was resuspended in HEM buffer (20 mM HEPES, 1.4 mM EGTA and 12.5 mM $MgCl_2$, pH 7.4) and 10% (v/v) glycerol for α_{1D}-AR; and TME buffer (50 mM Tris, 12.5 mM $MgCl_2$, 5 mM EGTA) and 10% (v/v) glycerol for α_{1A} and α_{1B}-ARs and the 5-HT_{1A}-R. All membranes were stored at −80 °C. Protein concentration was determined by using the Bradford reagent (Sigma, St Louis, MO, USA).

2.3. Radioligand binding assay

The reaction mixtures for all binding experiments were incubated at room temperature for 1 h, the reaction was terminated by the addition of PBS (4 °C) and vacuum filtration through GF/B filters (Whatman, Maidstone, UK). Radioactivity was measured by liquid scintillation counting.

2.3.1. α_1-AR binding

All ligands and membranes were suspended in HEM buffer. In saturation binding experiments, membranes containing each α_1-AR subtype were incubated with various concentrations of [^{3}H] prazosin (0.125–16 nM) in a total volume of 200 μL. For competition binding experiments, 1–4 μg of α_{1A} and α_{1B} -ARs and 10–32 μg of α_{1D} -AR membranes were incubated with 200 pM of [^{3}H] prazosin and increasing concentrations of test compounds in a total volume of 200 μL. Non-specific binding was defined as binding in the presence of 100 μM phentolamine.

2.3.2. 5-HT_{1A}-R binding

All ligands and membranes were suspended in 50 mM Tris-HCl and 4 mM $CaCl_2$, pH 7.4. In saturation binding experiments, membranes containing 5-HT_{1A}-R were incubated with varying concentrations of [^{3}H]-OH-DPAT (0.5–16 nM) in a total volume of 200 μL. In competition binding experiments, 6 μg of 5-HT_{1A}-R-containing membranes were incubated with 1 nM of [^{3}H]-OH-DPAT and increasing concentrations of test compounds in a total volume of 200 μL. Non-specific binding was defined as binding in the presence of 10 μM serotonin.

2.4. Inositol phosphate accumulation assays

Accumulation of total [^{3}H] inositol phosphates (IPs) was determined as described previously [11]. Briefly, 1 × 10^5 cells ml^{-1} of transiently transfected COS-1 cells were seeded into 96 well plates and cultured overnight with DMEM supplemented with 10% FBS. Cells were then washed with warmed PBS and labelled overnight with 10 μCi ml^{-1} [^{3}H] myo-inositol in inositol-free DMEM supplemented with 5% FBS. Cells were washed twice with 100 μL warmed PBS, and were treated for 45 min with fully-supplemented inositol-free DMEM containing 20 mM LiCl in the presence or absence of test compounds. An EC_{75} concentration of norepinephrine (10 μM) was then added for 30 min, and the reaction was terminated by addition of 0.4 M formic acid. Cells were lysed by freeze-thawing twice and were applied to AG 1-X8 columns. Total IPs were eluted with 1 M ammonium formate in 0.1 M formic acid. 200 μL of eluted sample was diluted into 1 mL ultra-pure water (Millipore, Billerica, MA, USA) and 4 mL Ultima-flow™ scintillation fluid (PerkinElmer, Waltham, MA, USA), and counted in a liquid scintillation counter.

2.5. Data analysis

Nonlinear regression analysis of saturation, competition binding, and inositol phosphate accumulation assay data was performed using the curve fitting program GraphPad Prism (San Diego, CA, USA). Inhibition constants (K_i) for each tested compound were determined by transformation of the program-calculated IC_{50} (concentration of ligand resulting in 50% inhibition of [^{3}H] prazosin or [^{3}H]-OH-DPAT) value using the Cheng–Prusoff equation, whereby $K_i = IC_{50}/1 + (L/K_D)$, where [*L*] is 200 pM [^{3}H] prazosin (α_1-ARs) or 1 nM [^{3}H]-OH-DPAT (5-HT_{1A}-R) and K_D is the dissociation constant. The competitive binding data for each ligand was tested for both one and two-site binding. A one-site binding model was determined as the appropriate form of analysis for all binding data. Statistically significant differences ($p < 0.05$)

between the affinities of all compounds were determined using one-way ANOVA and Student–Newman–Keuls multiple comparison tests.

2.6. Homology model

Homology models were built as previously described [12]. Briefly, sequences were aligned using CLUSTAL-W, following which the pairwise alignments were hand-edited to conform to the multiple sequence alignment, and also to ensure maximal overlap of conserved residues and minimal gaps in the helices and formation of the disulphide bond between C099 and C176. The human dopamine D_3 receptor (PDB ID-3PBL) crystal structure was used as the template [13] as the α_{1A}-AR has a higher sequence identity for D_3-R than the β-ARs, especially in the extracellular loops. The program MODELER [14] was used in its implementation in Accelrys Discovery Studio Client (DS) version 3.1 (Accelrys Software Inc. USA). The top ranked model was used in each case without further refinement.

2.7. Molecular docking

Possible binding sites of the compounds within α_{1A}-AR were predicted by docking these compounds into the α_{1A}-AR homology model using the program Genetic Optimization for Ligand Docking (GOLD) (Cambridge Crystallography Data Centre, UK). Hydrogens were added to all ligands and the receptor prior to performing the docking runs. All ligands were also protonated at the ring nitrogens prior to docking. To account for the diffuse nature of the resulting positive charge over the ring, no formal charge was assigned to the protonated nitrogen. The binding pocket was defined from the receptor cavity. Eight amino acids, known to interact with antagonists ($F86^{2.64}$ [1], $D106^{3.32}$, Q167 in extracellular loop 2 (ECL2), Q177 in ECL2, I178 in ECL2, N179 in ECL2, $F308^{7.35}$, $F312^{7.39}$) were defined as flexible side chains. The number of docking runs was set to 100, the "Detect Cavity" and "Early Termination" were set to be "False", and the "Flip Amide Bonds" and "Intramolecular Hydrogen Bonds" were set to be "True". All other parameters were left at their default values. The resulting docked poses are ranked according to score (highest scoring first). Gold scores, hydrogen bonds, and π-interactions of the ligands were analysed for the first pose in each selected cluster at a clustering distance of approximately 2–3 Å.

3. Results

3.1. The effect of linker length on affinity at α_1-ARs and the 5-HT_{1A}-R

The diquinolines with linker lengths from C2 to C12 (Fig. 1) were evaluated for ligand binding characteristics on membrane-expressed α_1-ARs and 5-HT_{1A}-R in competition radioligand binding experiments using [^{3}H] prazosin (α_{1A}-AR K_D = 0.21 nM, α_{1B}-AR K_D = 0.11 nM, α_{1D}-AR K_D = 0.37 nM) and [^{3}H]-OH-DPAT (K_D = 0.36 nM). The affinity of the two control compounds, phentolamine (pK_i: α_{1A}-AR 8.31 ± 0.13, n = 5; α_{1B}-AR 7.32 ± 0.15, n = 3; α_{1D}-AR 7.75 ± 0.08, n = 2) and serotonin (5-HT_{1A}-R, 8.85 ± 0.08, n = 3), are within the range of reported values [16,17].

All compounds tested display similar nanomolar affinity for α_{1A} and α_{1B} -ARs. The C2 compound has the highest affinity for both α_{1A} and α_{1B} -ARs, with K_i values of 25 and 52 nM, respectively. Compounds with linker lengths less than 7 showed 50- to 600-fold selectivity for α_{1A}-AR over 5-HT_{1A}-R and 4- to 30-fold selectivity over α_{1D}-AR (Table 1, Figs. 2 and 3). Those compounds with linker lengths greater than 7 have modest selectivity for α_{1A}-AR over 5-HT_{1A}-R (5- to 10-fold) (Table 1, Fig. 2). A similar linker length-affinity relationship is seen for each α_1-AR subtype, in that the affinity decreases as the chain length increases, reaching a nadir at 5 (α_{1A} and α_{1B} -AR) or 6 (α_{1D}-AR) carbon atoms; after which affinity increases as the linker is lengthened, peaking at 9 carbon atoms, and thereafter it decreases as the connecting chain is further lengthened. The C3 monoquinoline analogue (C3 amine) (see Fig. 1) shows significantly less affinity for each α_1-AR subtype compared to C3 diquinoline (Table 1), but the lack of the second 4-aminoquinoline ring did not significantly change the affinity for 5-HT_{1A}-R ($p > 0.05$) (Table 1). The addition of the 3 carbon linker onto 4-aminoquinoline (C3 amine) resulted in a significant increase in affinity for α_{1D}-AR, compared to 4-aminoquinoline ($p < 0.05$), but not the other receptors tested (Table 1).

3.2. Inhibition of NE-induced IP accumulation of the α_{1A}-AR by diquinolines

All compounds tested, phentolamine, C2, C7, and C9, completely inhibit the norepinephrine (10 μM) induced activation of α_{1A}-AR in a concentration dependent manner (Fig. 3), with the total IP accumulation data fitting a monophasic inhibition curve. Phentolamine has an IC_{50} of 0.5 μM (pIC_{50} 6.29 ± 0.08, n = 3). C2 is the most potent of the diquinolines tested, with an IC_{50} value of 2 μM, (pIC_{50} 5.71 ± 0.18, n = 3), with C7 displaying a similar IC_{50} of 3.5 μM (pIC_{50} 5.45 ± 0.06, n = 3) ($p > 0.05$). However, C9 which has similar affinity for α_{1A}-AR as C2, has an IC_{50} of 15 μM (pIC_{50} 4.82 ± 0.07, n = 3).

3.3. Docking of compounds into an α_{1A} homology model

4-Aminoquinoline, C2, and C9 diquinoline were docked to the inactive state α_{1A}-AR homology model, the binding pocket having been defined automatically as the receptor cavity. For all docked compounds, one of the 4-aminoquinoline moieties was situated within the orthosteric binding site, forming interactions with the typical orthosteric amino acids, such as $D106^{3.32}$. For the 4-aminoquinoline monomer, the two largest clusters (clustering at 2 Å) are within the orthosteric site, one interacting with the conserved $D106^{3.32}$, the other with Q177 in ECL2, via hydrogen bonds with the ring nitrogen (Fig. 4A, 4B). A cluster containing only 1 pose is located at the top of transmembrane helix two (TMII), TMIII and ECL2, forming π–π interaction with $F86^{2.64}$ (Fig. 4A, B). The largest cluster for C2 diquinoline (containing 14 poses at 2.7 Å) places the protonated nitrogen of one aminoquinoline moiety within hydrogen bond distance of $D106^{3.32}$ with the quinoline rings forming π–π interactions with $F289^{6.52}$ and $F312^{7.39}$ respectively, while the ring nitrogen of the second aminoquinoline forms a hydrogen bond with Q177 in ECL2 (Fig. 4C, D). Q177 has been shown to be responsible for α_{1A}-AR selectivity over α_{1B}-AR of the orthosteric antagonist phentolamine [18]. The first pose (highest scoring) in the first cluster (2 members at 2.7 Å) is located at a higher position than the largest cluster, with the bottom quinoline ring forming a π–π interaction with $F288^{6.51}$ and the other quinoline moiety interacting with extracellular residues, $F86^{2.64}$ and $W102^{3.28}$ (π–π) or ECL2 amino acids, R166 (π–cation) and C176 (hydrogen bond); while the second cluster which contains 3 poses has a hydrogen bond with $A103^{3.29}$ through the protonated nitrogen, and the other quinoline ring interacts with $F86^{2.64}$. Another pose located in a cluster containing 9 members interacts with $D106^{3.32}$, $F288^{6.51}$ and $F308^{7.35}$. The longer C9 homologue shows a different binding mode, with the poses within the largest cluster (14 members at 2.74 Å) indicating that one aminoquinoline interacts at the orthosteric site, forming

[1] Superscripts indicate the Ballesteros-Weinstein numbering scheme [15] here the first digit represents the transmembrane helix (TM) number followed by the position relative to the most conserved residue in each TM, assigned number 50. Numbers decrease towards the N-terminus.

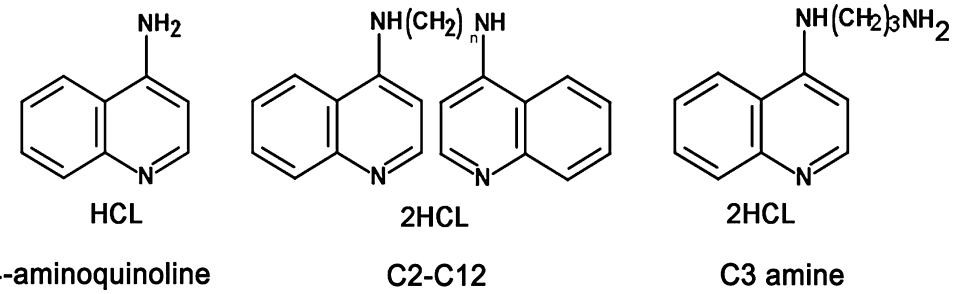

Fig. 1. Structures of the homobivalent 4-aminoquinoline compounds (diquinolines) tested. Diquinolines are referred to in the text as C_n-diquinoline, where *n* represents the number of methylene groups in the linking chain.

Table 1
Binding affinities for diquinolines at α_1-ARs and the 5-HT_{1A}-R.

	α_{1A}-AR			α_{1B}-AR			α_{1D}-AR			5-HT_{1A}-R		
	pK_i[a]	K_i[b] (nM)	*n*	pK_i[a]	K_i[b] (nM)	*n*	pK_i[a]	K_i[b] (nM)	*n*	pK_i[a]	K_i[b] (nM)	*n*
4-amino quinoline	4.64 ± 0.06	22,909	3	4.2 ± 0.28	63,096	3	4.26 ± 0.11	54,954	3	4.71 ± 0.43	19,498	3
C2	7.60 ± 0.26	25	5	7.28 ± 0.24	52	5	6.14 ± 0.01[c]	724	3	4.83 ± 0.38[c]	14,791	3
C3	7.29 ± 0.27	51	4	6.84 ± 0.14	145	5	6.32 ± 0.27[c]	479	3	5.45 ± 0.16[c]	3548	3
C5	6.53 ± 0.06	295	4	6.44 ± 0.05	363	3	5.93 ± 0.19[c]	1175	3	5.46 ± 0.09[c]	3467	4
C6	6.67 ± 0.20	214	5	6.54 ± 0.22	288	5	5.87 ± 0.04[c]	1349	3	5.03 ± 0.03[c]	9332	3
C7	6.69 ± 0.01	204	4	6.69 ± 0.51	204	3	6.30 ± 0.04	501	3	5.74 ± 0.41	1820	4
C8	6.91 ± 0.14	123	4	6.90 ± 0.17	126	3	6.53 ± 0.08	295	3	6.33 ± 0.15[c]	468	4
C9	7.27 ± 0.30	54	4	7.00 ± 0.12	100	3	6.93 ± 0.10	117	3	6.29 ± 0.17[c]	513	4
C10	6.58 ± 0.12	263	4	6.65 ± 0.07	224	4	6.40 ± 0.01	398	3	5.91 ± 0.11[c]	1230	4
C11	6.38 ± 0.04	417	4	6.26 ± 0.08	550	3	6.21 ± 0.09	617	3	5.62 ± 0.07[c]	2399	4
C12	6.07 ± 0.15	851	3	6.34 ± 0.07	457	3	5.04 ± 0.14[c]	9120	3	5.24 ± 0.03[c]	5754	3
C3 amine	5.21 ± 0.13[d]	6166	3	4.74 ± 0.30[d]	18,197	3	5.60 ± 0.11[d,e]	2512	3	4.80 ± 0.22	15,849	3

The data shown for each compound is the mean ± SE of separate assays, performed in triplicate.
K_i values were calculated according to the equation of Cheng and Prusoff. $K_i = IC_{50}/1 + ([L]/K_D)$ when [*L*] is the radioligand concentration and K_D its dissociation constant.
[a] Equates to the negative log of the K_i value.
[b] The concentration of ligand required to occupy 50% of all receptors if no radioligand were present.
[c] $p < 0.05$ compared to α_{1A}-AR.
[d] $p < 0.05$ compared to C3 diquinoline.
[e] $p < 0.05$ compared to 4-aminoquinoline.

interactions with F289$^{6.52}$, whilst the second quinoline moiety extends towards the extracellular surface of the receptor, interacting with F86$^{2.64}$ through π-π interaction, and forming a hydrogen bond with E87$^{2.65}$ (Fig. 4E, F). The binding modes of all three compounds are compared in Fig. 5.

4. Discussion

Adrenoceptors (ARs) were initially categorised into α and β subtypes in 1948 by Ahlquist, and in the 1970s the α-AR was further classified into α_1 and α_2 -ARs [19]. In 1986 α_1-ARs were successively subdivided into α_{1A} and α_{1B}–subtypes [20], and by the early 1990s the α_{1D}-AR subtype was recognised [10,21]. Prior to the characterisation of the three α_1-AR subtypes, the diquinolines examined in this study were shown to have high affinity for α_1-AR expressed in rat cerebral cortex and kidney [7,8]. The homologues with a linker length ≥4 displayed some selectivity for kidney α_1-ARs, which now may be interpreted as subtype selectivity of these compounds at the α_{1A} or/and the α_{1B}-AR, as it has been demonstrated that while all three α_1-AR are expressed in the rat brain, with the α_{1D}-AR being the predominant subtype, the α_{1D}-AR is absent from the rat kidney [22]. Our results extend, and

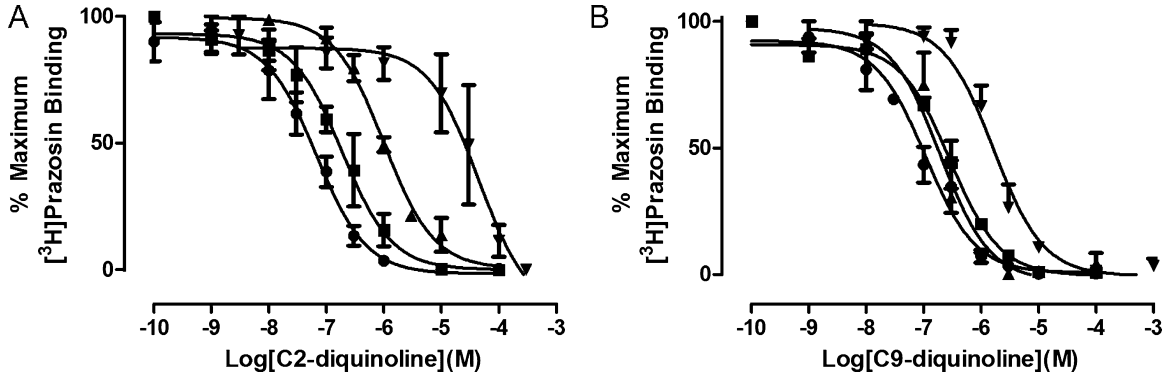

Fig. 2. Competition binding affinity of C2 and C9 diquinolines. Competition binding was performed on membranes prepared from α_{1A}, α_{1B}, α_{1D} -ARs or 5-HT_{1A}-R transfected COS-1 cells. The affinity of each compound was determined by its capacity to displace the binding of [^{3}H]-Prazosin (200 pM) from the α_{1A}-AR(●) α_{1B}-AR(■), α_{1D}-AR(▲) and the binding of [^{3}H]-OH-DPAT (1 nM) from the 5-HT_{1A}-R(▼) in separate experiments performed three to five times in triplicate. Points represent the mean percentage of maximum specific binding and vertical bars represent standard error. Curves were best fit to a single-site model.

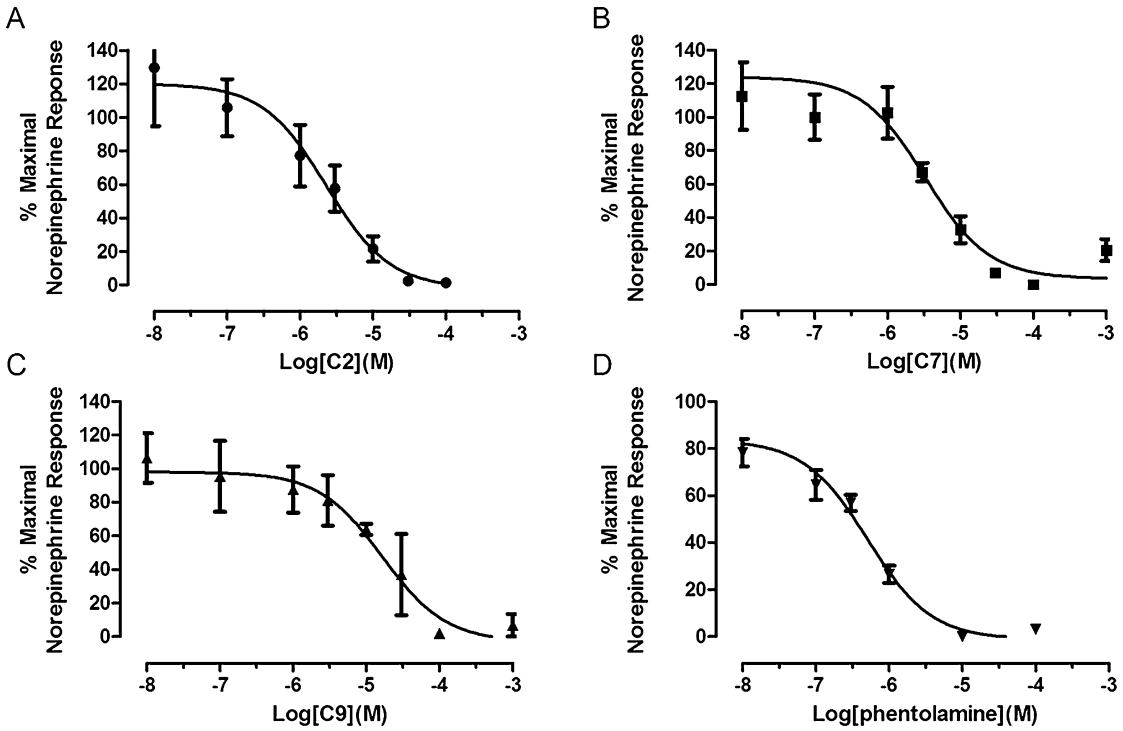

Fig. 3. Inhibition of norepinephrine induced total [^{3}H] inositol phosphate (IP) accumulation by diquinolines and phentolamine. Cells transiently transfected with α_{1A} adrenoceptor were incubated for 45 min at 37 °C with inositol free DMEM (10% FBS) containing 20 mM lithium chloride (LiCl) in the presence or absence of each tested compound, (A) C2, (B) C7, (C) C9, (D) phentolamine, after which 10 μM norepinephrine was added and the incubation continued for 30 min. Points represent the mean percentage of norepinephrine response and vertical bars represent standard error of separate experiments performed three to five times in triplicate. Curves best fit to a single-site model.

confirm, this inferred subtype selectivity for rat α_{1A} and α_{1B} -ARs over α_{1D}-ARs to the cognate human receptors for those compounds with a linker length less than 7. In addition, while 4-aminoquinoline shows no selectivity for α_{1A}-AR over 5-HT$_{1A}$-R, all the diquinolines, with the exception of C7, demonstrate selectivity for α_{1A}-AR over 5-HT$_{1A}$-R, with C2-C6 showing 12- to 590-fold selectivity and C7-C12 showing 4- to 9.5-fold selectivity. Furthermore, we confirm here that these compounds are antagonists for the α_{1A}-AR, supporting previous quoted unpublished results [7].

We hypothesise that the C2 diquinoline has the highest affinity due to its small size allowing favourable interactions within the catecholamine binding pocket and with ECL2 of the α_1-ARs. In contrast, the increased size of the C5-C7 diquinolines results in steric clashes leading to decreased affinity. However, when the chain length is further increased, to produce C9, it is now long enough to permit one of the quinoline moieties to interact favourably with residues in the extracellular region of the receptor, increasing affinity. Additional increases in linker length result in steric clashes within this extracellular domain, thereby decreasing affinity once more. This rationalisation for binding of the diquinoline series is consistent with the conceptual scheme described in the earlier work [7,8], but advances in knowledge of adrenoceptor structure now permit a more detailed proposal for the drug-receptor interactions involved, as described below.

The competition binding data suggest that the compounds are competing with prazosin for the same site, but they do not exclude the possibility of binding to two overlapping binding regions as has been proposed for other α_1-AR antagonists [23]. The docking of 4-aminoquinoline shows three regions of potential interaction, one which corresponds to the binding site of the endogenous ligands and includes an interaction with D106$^{3.32}$, the second corresponds to the upper extracellular part of the binding pocket of antagonists, such as phentolamine, and includes interaction with Q177 of ECL2, and the third is located within the extracellular region between TMII, TMIII, and ECL2, forming interaction with F86$^{2.64}$.

It has been suggested that unlike the binding of agonists, which occurs deeper within the binding pocket, antagonist binding involves further residues located in TMIII through TMVI, and that antagonists interact with amino acids which are localized closer to the extracellular surface of the receptors [18,24]. However, how known antagonists bind to the α_{1A}-AR still remains unclear due to the lack of detailed experimental structural knowledge. Site-directed mutagenesis studies have shown that three consecutive amino acid residues, Q177, I178, N179, which are located on ECL2 of the α_{1A}-AR, are responsible for the higher affinity for α_{1A}-AR over α_{1B}-AR for the antagonists phentolamine and WB4101 [18]. Related studies have shown that two phenylalanine residues (F308$^{7.35}$ and F312$^{7.39}$) in TMVII of the α_{1A}-AR are an important site for antagonist affinity [24]. Furthermore, F86$^{2.64}$ in TMII was demonstrated to be responsible for α_{1A} versus α_{1D} -AR selectivity of niguldipine [25]. These amino acid residues may also be responsible for the subtype selectivity of C2, C3, C5, C6 or/and C12 diquinolines for α_{1A}-AR over α_{1D}-AR or the 5-HT$_{1A}$-R.

Our results from docking C2 diquinoline into the α_{1A}-AR suggest that it forms a hydrogen bond with Q177 in ECL2 and a π-π interaction with F312$^{7.39}$ in TMVII: residues equivalent to T188 in the ECL2 and N386$^{7.39}$ in TMVII of the 5-HT$_{1A}$-R, respectively. C2 could also bind to A103$^{3.29}$ in TMIII which is I113$^{3.29}$ in the 5-HT$_{1A}$-R. These sequence differences in the two receptors may contribute to the selectivity of C2 diquinoline for the α_{1A}-AR over the 5-HT$_{1A}$-R. Furthermore, docking suggests that the C2 diquinoline could make π-interactions with W102$^{3.28}$ in TMIII, which is also a tryptophan (W121$^{3.28}$) in the α_{1B}-AR, but a valine (V171$^{3.27}$) in the α_{1D}-AR, and a phenylalanine (F112$^{3.28}$) in the 5-HT$_{1A}$-R. These docking results are consistent with our competition binding results, in which C2 has similar affinity for the α_{1A} and α_{1B}-ARs, and greater than 10-fold selectivity for α_{1A}-AR over α_{1D}-AR and the

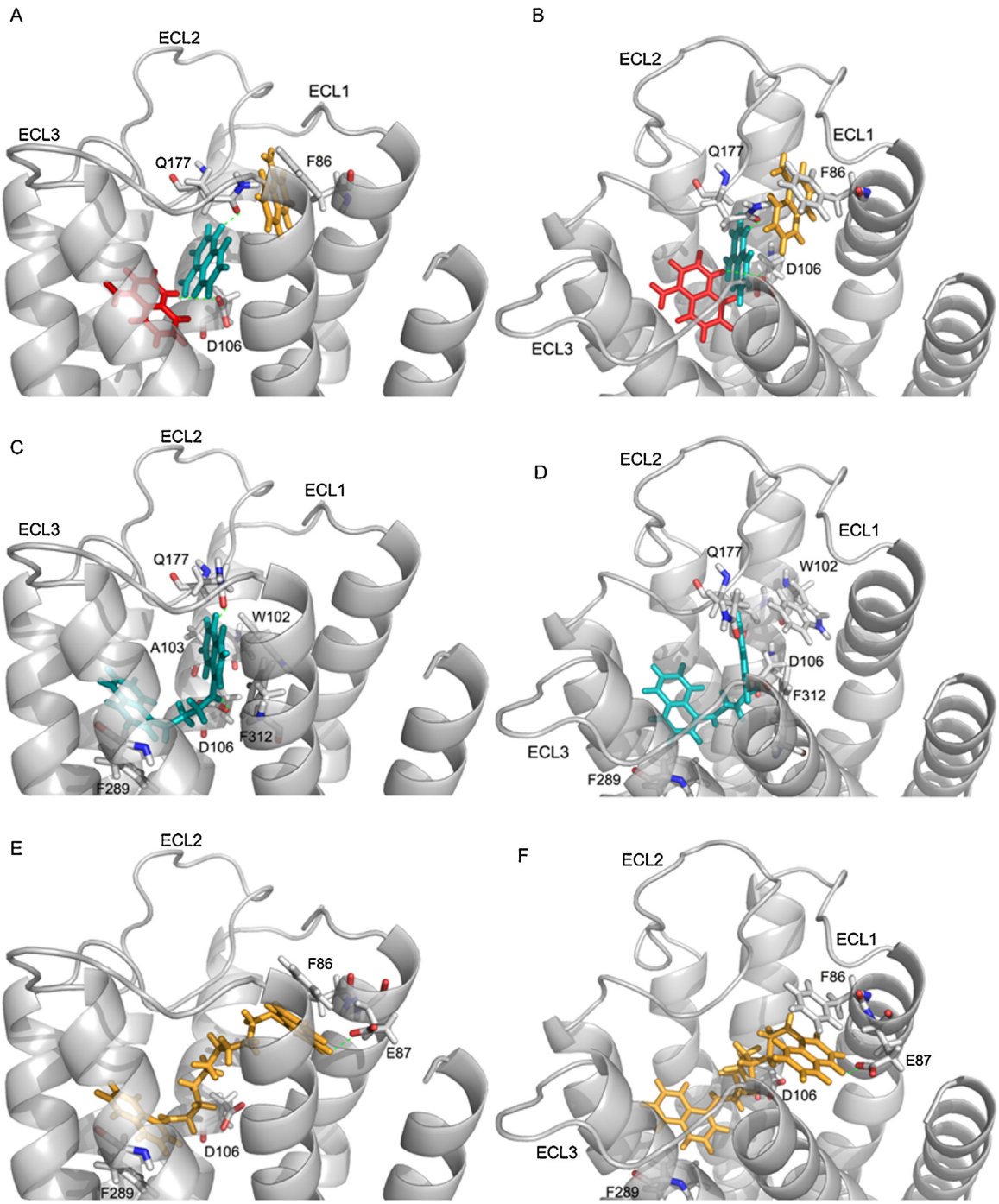

Fig. 4. Binding mode of 4-aminoquinoline (A & B), C2 (C & D), and C9 (E & F) in the α_{1A}-AR homology model and their main interactions. Each compound was docked into the α_{1A}-AR homology model based on a dopamine D_3 receptor crystal structure (3PBL). Two views are provided (A, C & E) a side-on view and (B, D & F) a top-down view, interacting amino acid side chains represented as light grey sticks with O atoms in red and N atoms in blue and hydrogen bonding represented by dashed lines. (A & B) Three main orientations of 4-aminoquinoline (first pose in each cluster) are represented in red, teal and gold; (C & D) The first pose in the largest cluster of C2 (teal), and two amino acids ($W102^{3.28}$ and $A103^{3.29}$) interacting with other poses are also represented. (E & F) The first pose in the largest cluster of C9 (gold) (For interpretation of the references to colour in this figure legend, the reader is referred to the web version of this article.)

5-HT_{1A}-R. Therefore $W102^{3.28}$ in TMIII of the α_{1A}-AR may be responsible for the selectivity of C2 diquinoline for the α_{1A}-AR. Additional π-interactions seen with the α_{1A}-AR in some poses, including $F86^{2.64}$ and $F308^{7.35}$, which are $Y96^{2.64}$ and $G382^{7.35}$ in the 5-HT_{1A}-R, respectively, could also result in the selectivity for the α_{1A}-AR over the 5-HT_{1A}-R. Taken together these results highlight a site formed by aromatic residues towards the top of TMII, TMIII and TMVII, which provides opportunities for aromatic π-interactions with ligands, generating α_1-AR subtype selectivity without 5-HT_{1A}-R off-target affinity.

The docking results indicate that the quinoline 4-amino group, as well as the protonated ring nitrogen, can form hydrogen bonds with the receptor, whilst the quinoline moiety participates in π–π interactions. That both quinoline groups contribute significantly to ligand binding to α_1-ARs is confirmed by the finding that the analogue with only one quinoline system, but two amino groups at both ends of a C3 linker (C3 amine, Fig. 1), has reduced affinity at each α_1-AR subtype compared to its equivalent diquinoline.

The docking results for 4-aminoquinoline and C9 diquinoline, when taken together, draw attention to a region of α_1-ARs, a site

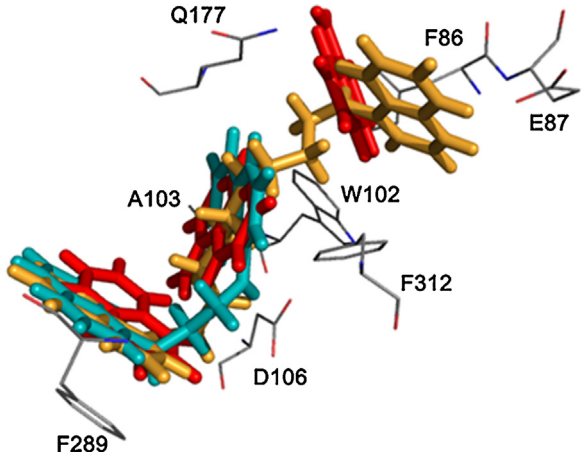

Fig. 5. Main interacting α_{1A}-AR sidechains identified through docking of 4-aminoquinoline (red), C2 (teal), and C9 (gold) with the α_{1A}-AR homology model. Sidechains are represented by sticks coloured by element; oxygen, red; nitrogen, blue, carbon, black (For interpretation of the references to colour in this figure legend, the reader is referred to the web version of this article.)

formed by residues at the top of TMII ($F86^{2.64}$ and $E87^{2.65}$), which provides opportunities for aromatic π-interaction or hydrogen bonding. Whilst C9 diquinoline has an affinity similar to that of C2 diquinoline, it lacks the α_{1A}/α_{1B} -AR selectivity over α_{1D}-AR of C2 diquinoline, and is only 9.5-fold selective against 5-HT_{1A}-R. This may be accounted for by the conservation of $E^{2.65}$ across all three α_1-ARs and the conservative substitution of a $Q^{2.65}$ in 5-HT_{1A}-R. In contrast, $F86^{2.64}$ is not conserved across all three α_1-ARs and has previously been suggested to contribute to the α_{1A} versus α_{1D} -AR selectivity of niguldipine [25] which was not seen with C9 diquinoline. Overall, C9 diquinoline forms fewer specific bonding interactions with the receptor in comparison to C2 diquinoline; this may suggest that the longer linker is contributing to the overall affinity due to hydrophobic interactions.

The contribution of the longer linkers to hydrophobic interactions with the studied receptors has not been determined. C3 amine has significantly increased affinity compared to 4-aminoquinoline itself only at α_{1D}-AR, but not the other receptors tested, so we can speculate that a three carbon linker may not be long enough to contribute significant hydrophobic interactions. However, the longer methylene linker may contribute to ligand affinity, as the docking suggests that the binding pocket surrounding the C9 linker-region is predominately hydrophobic. Other studies investigating bivalent ligands have shown that the addition of the linker alone can increase ligand affinity, such as the addition of a 13-atom linker to the dopamine D_2 receptor antagonist clozapine or a 7-atom linker added to muscarinic M_2 receptor antagonists 3-benzhydryl pyrrolidine and 4-aminobenzylpiperidine [26,27]. However, this is not a universal effect, as a homovalent morphinan ligand with a 14-atom tail showed decreased opioid receptor affinity compared to the parent compound [28].

Several studies of bivalent ligands have shown increased affinity following the attachment of a second pharmacophore with a bridging linker. It has been suggested in studies of the opioid and 5-HT_4 receptors, that this increased affinity is due to the bivalent compound binding to adjacent receptors [29,30]. However, the compounds in question all have linkers 20 to 66 atoms in length. It has been suggested that a linker of 26 atoms is required to bind across a GPCR dimer [31], significantly longer than the 9 methylene linker that gives optimal bivalent affinity in the present work. Furthermore, our docking study would suggest that receptor cross-linking is not the mechanism of increased affinity seen with the homobivalent 4-aminoquinoline compounds, as the overall length of the even the longest compound is not sufficient to bind to the orthosteric binding site of α_{1A}-AR and significantly protrude from the top of the receptor. Interestingly, a study in which a muscarinic antagonist and a β_2-adrenoceptor agonist were linked, also found that 9 atoms was the optimal linker length for increased β_2-adrenoceptor affinity [32]. In addition, a study of homobivalent morphinan ligands with linkers of 4 and 10 atoms produced high affinity for opioid receptors, but linkers of 5–9 and more than 10 atoms in length had reduced affinity [28]; a similar pattern to that seen with the homobivalent 4-aminoquinolines with linkers of 2 and 9 atoms providing the best affinity profile.

In summary, the limited α_{1D}-AR and 5-HT_{1A}-R and high α_{1A}-AR affinity of the diquinolines studied here makes them promising leads for future drug development of α_{1A}-AR selective ligands. Furthermore, these diquinolines can be used as a molecular ruler to investigate the location of novel extracellular binding sites on the α_{1A}-AR.

Acknowledgments

JC acknowledges the financial support of the China Scholarship Council.

References

[1] Beduschi MC, Beduschi R, Oesterling JE. Alpha-blockade therapy for benign prostatic hyperplasia: from a nonselective to a more selective alpha1A-adrenergic antagonist. Urology 1998;51:861–72.
[2] Sarma PK, Tiwari A, Pal A. α1-adrenoceptors as potential therapeutic targets. Expert Opin Ther Pat 2005;15:1333–51.
[3] Rudner XL, Berkowitz DE, Booth JV, Funk BL, Cozart KL, D'Amico EB, et al. Subtype specific regulation of human vascular alpha(1)-adrenergic receptors by vessel bed and age. Circulation 1999;100:2336–43.
[4] Andersson KE, Wyllie MG. Ejaculatory dysfunction: why all alpha-blockers are not equal. BJU Int 2003;92:876–7.
[5] Borbe HO, Metzenauer P, Szelenyi I. 5-HT1a-Agonistic properties of naftopidil, a novel antihypertensive drug. Eur J Pharmacol 1991;205:105–7.
[6] Palea S, Chang DF, Rekik M, Regnier A, Lluel P. Comparative effect of alfuzosin and tamsulosin on the contractile response of isolated rabbit prostatic and iris dilator smooth muscles – possible model for intraoperative floppy-iris syndrome. J Cataract Refr Surg 2008;34:489–96.
[7] Adams A, Jarrott B, Denny WA, Wakelin LPG. Differences between central and peripheral rat α-adrenoceptors revealed using binuclear ligands. Eur J Pharmacol 1986;127:27–35.
[8] Adams A, Jarrott B, Elmes BC, Denny WA, Wakelin LP. Interaction of DNA-intercalating antitumor agents with adrenoceptors. Mol Pharmacol 1985;27:480–91.
[9] Lopata MA, Cleveland DW, Sollnerwebb B. High-level transient expression of a chloramphenicol acetyl transferase gene by DEAE-dextran mediated DNA transfection coupled with a dimethylsulfoxide or glycerol shock-treatment. Nucleic Acids Res 1984;12:5707–17.
[10] Perez DM, Piascik MT, Graham RM. Solution-phase library screening for the identification of rare clones: isolation of an alpha 1D-adrenergic receptor cDNA. Mol Pharmacol 1991;40:876–83.
[11] Chengalvala M, Kostek B, Frail DE. A multi-well filtration assay for quantitation of inositol phosphates in biological samples. J Biochem Bioph Meth 1999;38:163–70.
[12] Kufareva I, Rueda M, Katritch V, Stevens RC, Abagyan R, Participants GD. Status of GPCR modeling and docking as reflected by community-wide GPCR dock 2010 assessment. Structure 2011;19:1108–26.
[13] Chien EYT, Liu W, Zhao QA, Katritch V, Han GW, Hanson MA, et al. Structure of the human dopamine D3 receptor in complex with a D2/D3 selective antagonist. Science 2010;330:1091–5.
[14] Sali A, Potterton L, Yuan F, van Vlijmen H, Karplus M. Evaluation of comparative protein modeling by MODELLER. Proteins 1995;23:318–26.
[15] Ballesteros JA, Weinstein H. Integrated methods for the construction of three dimensional models and computational probing of structure–function relations in G-protein coupled receptors. Methods Neurosci 1995;25:366–428.
[16] Newmantancredi A, Wootton R, Strange PG. High-level stable expression of recombinant 5-HT1a 5-hydroxytryptamine receptors in chinese-hamster ovary Cells. Biochem J 1992;285:933–8.
[17] Shibata K, Foglar R, Horie K, Obika K, Sakamoto A, Ogawa S, et al. KMD-3213, a novel, potent, alpha(1a)-adrenoceptor-selective antagonist – characterization using recombinant human alpha(1)-adrenoceptors and native tissues. Mol Pharmacol 1995;48:250–8.
[18] Zhao MM, Hwa J, Perez DM. Identification of critical extracellular loop residues involved in alpha(1)-adrenergic receptor subtype-selective antagonist binding. Mol Pharmacol 1996;50:1118–26.

[19] Dubocovich Ml Langer SZ. Negative feedback regulation of noradrenaline release by nerve-stimulation in perfused cats spleen - differences in potency of phenoxybenzamine in blocking presynaptic and post-synaptic adrenergic-receptors. J Physiol – London 1974;237:505–19.
[20] Morrow AL, Creese I. Characterization of alpha-1-adrenergic receptor subtypes in rat-brain – a reevaluation of [^{3}H] WB4104 and [^{3}H] prazosin binding. Mol Pharmacol 1986;29:321–30.
[21] Piascik MT, Smith MS, Soltis EE, Perez DM. Identification of the messenger-RNA for the novel alpha(1d)-adrenoceptor and 2 other alpha(1)-adrenoceptors in vascular smooth-muscle. Mol Pharmacol 1994;46:30–40.
[22] Rokosh DG, Bailey BA, Stewart AFR, Karns LR, Long CS, Simpson PC. Distribution of alpha-1c-adrenergic receptor messenger-RNA in adult-rat tissues by RNase protection assay and comparison with alpha-1b and alpha-1d. Biochem Bioph Res Co 1994;200:1177–84.
[23] Mcgrath JC. Evidence for more than one type of post-junctional alpha-adrenoceptor. Biochem Pharmacol 1982;31:467–84.
[24] Waugh DJJ, Gaivin RJ, Zuscik MJ, Gonzalez-Cabrera P, Ross SA, Yun J, et al. Phe-308 and Phe-312 in transmembrane domain 7 are major sites of alpha(1)-adrenergic receptor antagonist binding - Imidazoline agonists bind like antagonists. J Biol Chem 2001;276:25366–71.
[25] Hamaguchi N, True TA, Saussy DL, Jeffs PW. Phenylalanine in the second membrane-spanning domain of alpha(1A)-adrenergic receptor determines subtype selectivity of dihydropyridine antagonists. Biochemistry 1996;35:14312–17.
[26] McRobb FM, Crosby IT, Yuriev E, Lane JR, Capuano B. Homobivalent ligands of the atypical antipsychotic clozapine: design, synthesis, and pharmacological evaluation. J Med Chem 2012;55:1622–34.
[27] Steinfeld T, Mammen M, Smith JAM, Wilson RD, Jasper JR. A novel multivalent ligand that bridges the allosteric and orthosteric binding sites of the M-2 muscarinic receptor. Mol Pharmacol 2007;72:291–302.
[28] Neumeyer JL, Zhang A, Xiong WN, Gu XH, Hilbert JE, Knapp BI, et al. Design and synthesis of novel dimeric morphinan ligands for kappa and mu opioid receptors. J Med Chem 2003;46:5162–70.
[29] Mathews JL, Peng XM, Xiong WA, Zhang A, Negus SS, Neumeyer JL, et al. Characterization of a novel bivalent morphinan possessing kappa agonist and mu agonist/antagonist properties. J Pharmacol Exp Ther 2005;315:821–7.
[30] Russo O, Berthouze M, Giner M, Soulier JL, Rivail L, Sicsic S, et al. Synthesis of specific bivalent probes that functionally interact with 5-HT4 receptor dimers. J Med Chem 2007;50:4482–92.
[31] Soriano A, Ventura R, Molero A, Hoen R, Casado V, Cortes A, et al. Adenosine A(2A) receptor-antagonist/dopamine D(2) receptor-agonist bivalent ligands as pharmacological tools to detect A(2A)-D(2) receptor heteromers. J Med Chem 2009;52:5590–602.
[32] Steinfeld T, Hughes AD, Klein U, Smith JAM, Mammen MTHRX-198321. Is a bifunctional muscarinic receptor antagonist and beta(2)-adrenoceptor agonist (MABA) that binds in a bimodal and multivalent manner. Mol Pharmacol 2011;79:389–99.